

A Hybrid Approach to Wide-Baseline Image Matching

Rahul Mitra

Indian Institute of Technology, Bombay

mitter@cse.iitb.ac.in

Sharat Chandran

Indian Institute of Technology, Bombay

sharat@cse.iitb.ac.in

Jiakai Zhang

New York University

zhjk@nyu.edu

Arjun Jain

Indian Institute of Technology, Bombay

ajain@cse.iitb.ac.in

Abstract

Recent works such as [9, 15] have proposed the learning of robust local image descriptors using a Siamese convolutional neural network directly from images instead of hand-crafting them like traditional descriptors such as SIFT [7] and MROGH [3]. Though these algorithms show the state-of-the-art results on the Multi-View Stereo (MVS) [12] dataset, they fail to accomplish many challenging real world tasks such as stitching image panoramas, primarily due to the limited performance of finding correspondence.

In this paper, we propose a novel hybrid algorithm with which we are able to harness the power of a learning based approach along with the discriminative advantages that traditional descriptors have to offer. We also propose the *PhotoSynth* dataset, with size of an order of magnitude more than the traditional MVS dataset in terms of the number of scenes, images, patches along with positive and negative correspondence. Our *PhotoSynth* dataset also has better coverage of the overall viewpoint, scale, and lighting challenges than the MVS dataset. We evaluate our approach on two data sets which provides images having high viewpoints difference and wide-baselines. One of them is Graffiti scene from the Oxford Affine Covariant Regions Dataset (ACRD) [8] for matching images with 2D affine transformations. The other is the Fountain-P11 dataset [11] for images with 3D projective transformations. We report, to the best of our knowledge, the best results till date on the ACRD Graffiti scene compared to descriptors such as SIFT, MROGH or any other learnt descriptors such as [9].

1. Introduction

Designing high quality descriptors for local image patches is important for many computer vision tasks such as

structure from motion(SFM) [10], stitching image panoramas [2], wide baseline matching [11] and tracking [6, 1]. In these tasks, local image descriptors are typically used to find correspondence among images based on the distance of the image descriptors.

A successful image descriptor should be able to satisfy the two conflicting constraints of a) having sufficient discriminative power between semantic content for use in general vision tasks, while b) remaining invariant to transformations in the input space that obfuscates patch correspondence. Since invariance is inversely proportional to discriminative power [8], many state-of-the-art image descriptors have been designed [7, 3, 1] or optimized [12] to find a good balance between these conflicting constraints. Due to the complexity of the task, more recent methods [9, 15] propose to train a convolutional neural network (ConvNet) to learn the descriptors directly from the image patches. The data they use to train the ConvNet is the Multi-View Stereo (MVS) dataset [12] which contains millions of image patches. The ConvNet based descriptors provide significantly improved performance when evaluated on the MVS dataset. However they perform poorly in finding the point correspondences in images that occur in real scenarios with large scale and viewpoint variation as shown in Sec. 7.

There are two main reasons for such low performance. First the MVS dataset contains only three scenes and does not provide sufficient variation in terms of scene content, viewpoint, and scale. (We note here that a scene consists of a large number of images.) Hence the descriptors computed from these models do not generalize well. To improve the quality of training data, in this paper, we introduce a new *PhotoSynth* dataset which has 15 scenes with a large variety in terms of scene content. Furthermore, there are significantly more variations among the pairs of patches in terms of viewpoint and scale as compared to the MVS dataset, which makes our dataset more challenging and at the same

time can be used for learning more robust and generic descriptors.

Secondly, even with a dataset having sufficient variations in content and geometry, it is hard to train a descriptor using ConvNet to embed both structural information using large context windows and statistical information using small context windows. For instance, non-matching patches may have similar structure features but different local statistical information so the ConvNet based approach cannot distinguish the difference.

To address this issue we propose a novel hybrid approach to combine both the ConvNet based descriptor and the heuristic descriptor like MROGH or SIFT. We train the ConvNet descriptor to embed only global structure information. This is achieved by ignoring non-matching pairs that have very similar structural information. A more detailed explanation is provided in Sec. 6. Then, in order to distinguish the actual correspondence patch from structurally similar patches, we first use ConvNet descriptor to find a number of potential matches having similar structure and then use a heuristic descriptor like MROGH to determine the correct match from them. This hybrid matching approach is found to perform much better than the state of the art while matching images with viewpoint differences.

We use the *graffiti* scene from the ACRD dataset [8] and the fountain-P11 [11] for comparing our model with hybrid matching against other popular descriptors. The *graffiti* scene is chosen as it has images with very high variations in viewpoint and scale similar to one which is encountered sufficiently often in real world images-in-the-wild situation. The p11-fountain scene has a set of images which have wide base lines.

The main contributions of our paper therefore are:

- The *PhotoSynth* dataset which has 15 different scenes and high geometric and photometric variations among images compared to the traditionally available MVS dataset.
- A novel hybrid matching technique for finding point correspondences. We believe such a ‘dual’ paradigm approach may be increasingly useful in other learning-based solutions.

2. Related Work

The most commonly used dataset to train ConvNet based models for image descriptors is the MVS dataset. It uses the structure from motion (SFM) [10] paradigm to create 3D point clouds and camera poses from a large collection of images taken from a scene. The reconstruction is done using SIFT detectors and descriptors [7]. In older versions of the MVS dataset [4], patches around re-projections of the 3D point into images are used to create ground truth correspondences. The patches are scale and orientation nor-

malized. However, due to re-projection error there is noise in the matching and non-matching pairs in the dataset, and hence accuracy poses a limitation.

The newer version of the MVS dataset [12] uses dense reconstruction via SFM to generate more accurate correspondences. To generate these correspondences, a local dense sample of points around an interest point (p_1) in an image is projected into a second image via the dense point cloud and the method of least squares is used to estimate the position, rotation and scale of p_2' , the projection of p_1 in the second image. The nearest neighbor among all true interest points in the second image p_2' which lie between 5 pixels in position, 0.25 octaves in scale and $\pi/8$ in rotation are considered a match. This dataset has 3 scenes including Liberty(LY), Notredame(ND) and Yosemite(YO) with 450,092, 468,159 and 633,587 patches. Each scene is also provided with a list of pairs of size 100,000, 200,000 and 500,000 and with 50% matching and 50% non-matching pairs.

However, the MVS dataset has only three scenes and there is not sufficient variation in terms of scene content, viewpoint and scale. Further the non-matching pairs provided in the lists have far too less overlapping information. On the test, this makes them easier to discriminate than those pairs which occurs while finding point correspondences in real scenarios. As evidence for this proposition, in Sec. 7, we show that models trained using this dataset perform poorly in the evaluation on both ACRD and our *PhotoSynth* dataset.

3. PS Dataset

The PhotoSynth-based dataset (PS) has 15 scenes with considerable variation in content. Each scene consists of an average of approximately 250 color images, and a corresponding sparse 3D point cloud created using SFM [13, 14]. The number of patches per scene is of course much larger (approximately 60,000 to 100,000 per scene). Image patches are created by defining a square neighborhood around the projections of 3D points in the images. The SFM process provides correspondences having wide baselines which otherwise are not possible to obtain by stereo matching using SIFT or other heuristic descriptors. Hence, a descriptor model trained on such wide correspondences is expected to out-perform heuristic descriptors like SIFT.

Significantly, in order to capture extreme viewpoint differences potentially exhibited by scenes in the wild, we also create 10 additional images of several flat surfaces. Each such image is considered as a scene in keeping with the rest of the nomenclature. In such a scene, we form pairs by taking a patch from the image and an affine transform of it. Details on forming such pairs are contained in Sec. 5. Representative images of a few scenes from our dataset is shown in Fig. 1. The last two rows are scenes from our test

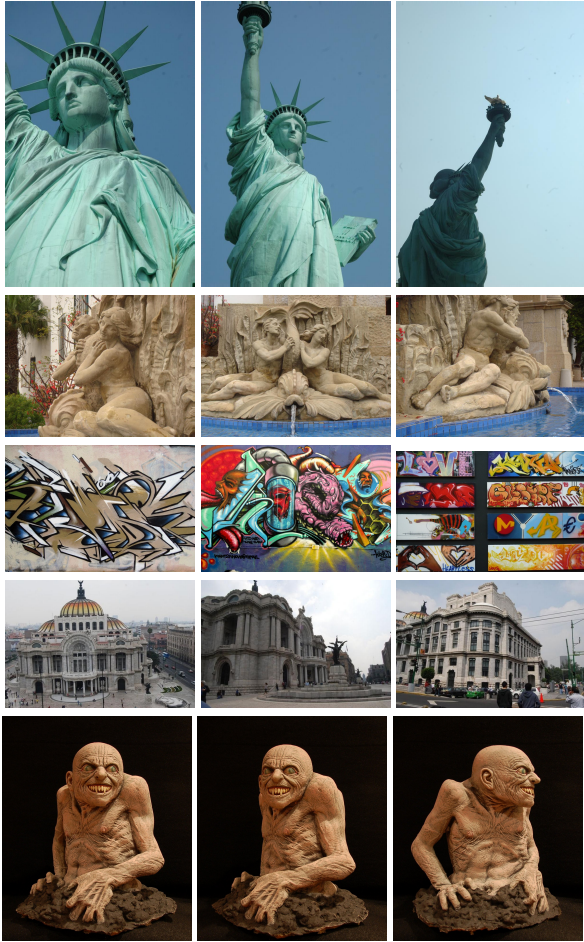


Figure 1. Sample images of scenes from our PS dataset. The first 3 rows are scenes taken from our training set and the last 2 rows are from the test set. The third row shows 3 out of the 10 images used for creating affine transform pairs. As can be seen, these images have large variations in terms of baseline and pose.

set and is used in evaluation in Sec. 7.

Let us denote the set of all the patches belonging to a 3D point i be P_i . To control scale variations among P_i , the ratio $s = f/d$ is calculated for each patch. Here, f is the focal length of the camera corresponding to the image the patch was taken and d is the distance between the camera center and the 3D point projected along the camera's view direction. Now, for every 3D point i , the median s'_i from the set P_i is calculated and only a subset of patches P'_i are retained whose $0.5s'_i \leq s \leq 2s'_i$. Next, for every patch in P'_i its relative scale(rs) is calculated as the ratio between s of a patch and $\min_{P'_i} s$. To add variations among the patches in terms of scale, each rs for a patch is modified by randomly multiplying by a number between $[0.8, 1.2]$. Square patches of size $64 * rs$ are cropped from images and then scaled back to 64.

To ensure the variations in viewpoints among the patches

coming from the same 3D point, we use the angle(v) formed by the viewing directions of their respective cameras. We sample a subset of these patches such that every pair in the set v lies between two thresholds. The lower threshold varies slightly for different scenes from 10 degrees to 15 degrees. The upper threshold is kept at 120 degrees.

To ensure compliance with the earlier methods, the format of our PS dataset is the same as that of the MVS dataset. Each scene contains a large number of 64×64 pixels RGB patches stacked row major wise to grids of 16 rows and columns. These grids are then saved as images of size 1024×1024 pixels ($1024 = 64 * 16$). When training our model we convert the RGB patches into grayscale so that we can compare with other descriptors during evaluation. Each scene is provided with a patch information list with an entry for all the patches in that scene. The information list contains 3D point index to which the patch is belongs, the grid image id where the patch is located and the (x,y) co-ordinates of the center of the patch in the grid image. Finally, each scene also contains a match-list containing pair of indices from the information list of all the matching pairs. The number of matching pairs in a scene varies from 60,000 to 100,000. For training we use 12 scenes out of 15 and the rest as test scenes. The test scenes have an additional list containing randomly selected 25,000 matching and 25,000 non-matching pairs. Sample patches from our dataset are shown in Fig. 2.

A comparison between the variations in patches found in the MVS dataset with ours is shown in Fig. 2. We can see variations in view point and scale between the pairs in our case compared to the MVS dataset. Later in Sec. 7 we show the inferior performance of models trained on MVS compared to our dataset.

4. Model

We use the Siamese Network as used by Hadsell et al. [5]. To make the model more invariant to scale variations we use multi-resolution image patches as the input to the ConvNet. Our network has 3 channels as shown in Fig. 3 and accepts patches of size 64×64 pixels. The first channel takes the entire patch. The second channel takes a 32×32 pixels patch cropped around the center and scaled to 64×64 pixels. Similarly the third channel takes a central 16×16 pixels patch and scaled to 64×64 pixels. Each channel has identical structure of two convolution layers of 128 features with average pooling of stride 2 and shares the parameters as shown in Fig. 5. The output maps from the 3 channels are then added to form one channel and passed through 3 convolution layers of 64 features each. The result is then flattened to form a 1D tensor ($64 * 16 * 16 = 16,384$) size and passed through fully connected layers of size 1024 and 128. The last layer of the fully connected layer is the dimension of our descriptor. We have also used batch nor-

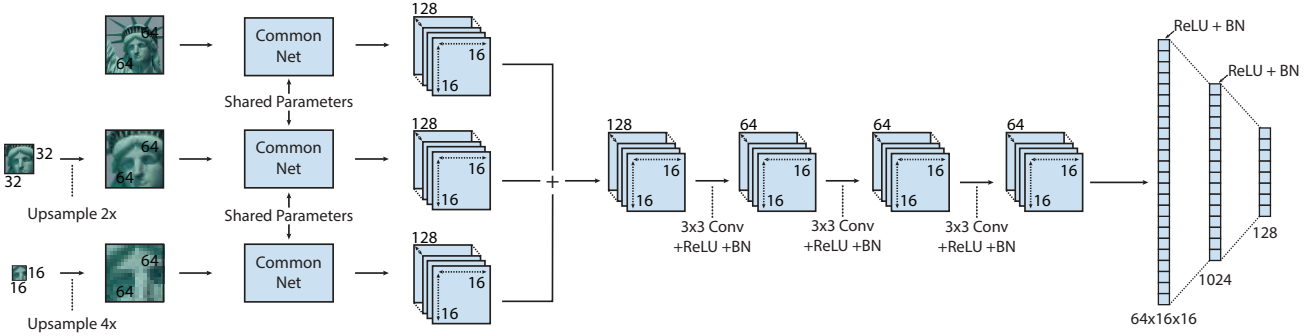


Figure 3. Our Model

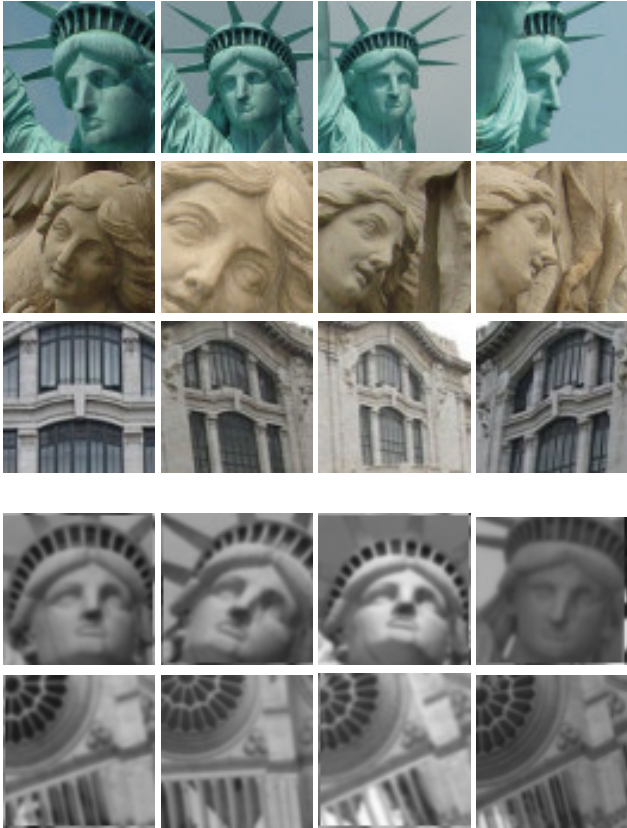


Figure 2. Top three rows are examples of corresponding patches from our PS dataset, the bottom two rows are sample patches from the MVS dataset. As it can be seen, the PS dataset includes patches which have much larger variations as compared to the MVS dataset.

malization after every convolution and fully connected layer except the output layer to speed up training.

5. Learning

To train our network we use the *contrastive* loss function used in [5] and shown in Eq. 1. Here D_w is the output of



Figure 4. Shows a different affine transformation for a given patch. The left most patch is the non-transformed base patch and other three are random affine transformations.

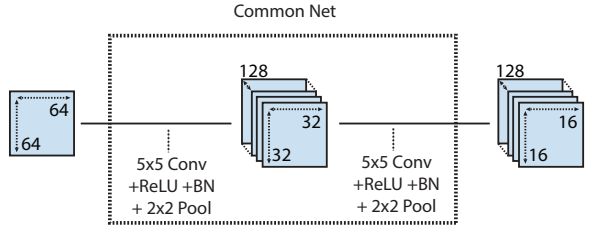


Figure 5. Common Net

the network for when its parameters are W . Y is 1 when the pair AB forms a match and 0 otherwise. m is the margin by which a non-matching pair should differ in the descriptor distance.

$$L(W, Y, A, B) = (Y) \frac{1}{2} (D_w)^2 + (1 - Y) \frac{1}{2} \{ \max(0, m - D_w) \}^2 \quad (1)$$

Our batch size consists of 64 pairs and we train 2,000 batches per epoch. Out of the 64 pairs, 16 pairs are matching and the rest are non-matching. For the first epoch since the parameters are randomly initialized we sample the matching and non-matching pairs at random. Second epoch onwards we use mining strategies in selecting matching and non-matching pairs. For each scene, we divide its matching pairs into 4 buckets according to descriptor distance obtained by current model. The first bucket contains the closest and the last contains the farthest. For each epoch we then sample the required list of positive pairs from the buckets in the ratio 1:2:5:8.

To create non-matching pairs, we take a subset of patches(S) from all the patches(N). For every patch(p) in

we divide N patches into 4 buckets (first one being closest and last one being farthest in terms of descriptor distance) and sample 5 patches from the first two buckets in the ratio 4:1 and form non-matching pairs with p. We ensure that we don't pair any of matching patches as non-matching. When selecting non-matching patches for p from the first bucket, we first try to select those patches which lie in an image where p forms a matching pair and with distance less than that matching pair. If no such pairs are found then we choose at random from the bucket. We keep a hash table to remove duplicate pairs. From this list of non-matching pairs we randomly select the required negatives for the epoch.

To reduce over-fitting, we perturb the patches before passing them through the network. The perturbations include rotating and scaling the patch with random values within the range $[-\pi/6, +\pi/6]$ and $[1.0, 1.1]$ respectively.

We also use perturbations to create matching and non-matching pairs from the single image scenes. A matching pair is formed by pairing a patch and an affine transformation of it similar to Fig. 6. For non-matching pairs, a patch is paired with an affine transformation of some other patch from the same single image. We accomplish this by taking a patch of three times the size (192 pixels in our case) required by the network and assign new positions to its four corner points. The difference in the positions are limited to be within a fixed range. For instance, if the patch is of 192 pixels and the bottom left corner is $(0, 0)$ and top right corner is $(192, 192)$ then its new positions will lie within $([-10, 75], [-10, 30])$ and $([80, 150], [90, 150])$ respectively. Using these 4 new positions, we calculate the affine transformation matrix. After the transformation, we crop out the 64×64 pixels patch around the point obtained by transformation of the center point in the original patch. The original patch is taken 3 times the size required by our network so as to avoid border artifacts while cropping the smaller 64×64 pixels patch. Fig. 4 shows different transformation of a single patch.

6. Hybrid Matching

In the process of training our model, we have observed that our model does not perform well when we have non-matching pairs sharing a lot of structural information but having difference in local statistical information. This happens when for a non-matching pair $[A, B]$, the center of B lies very close to the point correspondence of A . One explanation for this is that training objective becomes very difficult when we have to capture both the structure information and local statistical information. Larger patches provides better structural information but poor local statistical information while smaller patches capture better local statistical information. Among the two alternatives, we choose a model that is better at capturing structural information. This is achieved by ignoring non-matching pairs like $[A, B]$

mentioned earlier while training. Using such a model, for a patch in an image, we can filter out patches having similar structural information in the other image. However, its nearest neighbor may not be the correspondence point as it does not discriminate local statistics well. In Fig. 6 we see top 5 nearest neighbors obtained from our model for point marked in green in the left image as points marked in red in the right image. The correct correspondence in the right image is also marked as green and hence have both red and green markings. We can see that our top 5 nearest neighbors are either the actual correspondence point itself or lie in a small zone around the correspondence point or have similar structural information. In the bottom half of the figure, the left patch marked in green correspond to the green point in the left image. The row of patches marked as red comes from their corresponding to the red points. The patches are arranged left to right in increasing order distance. The second patch from the left is the correct correspondence and is also marked with green and corresponding to green point in the right image. Now, using descriptor like MROGH which is better at discriminating local statistics, we can match only within these filtered out patches to get the correct correspondence. In Fig. 6 the blue points in the right image shows the top 5 nearest neighbors using MROGH which are clearly inferior at matching structural information. However when using just the red patches for selecting a match we get correct patch as the nearest neighbor.

This hybrid matching scheme leads to matching more numbers of correct correspondences as shown later in Sec. 7. We use the distance-ratio (explained in Sec. 7) method for matching.

7. Results

In this section we evaluate our model with hybrid matching against DeepDesc [9] and DeepCompare [15] and other popular descriptors. DeepCompare provides us with two architectures. The first one is the 2-channel network that directly outputs a score that quantifies similarity between a pair of patches without computing intermediate descriptors. The second is a two-resolution Siamese network that given a pair of patches computes its descriptors and uses an additional decision network to compute similarity score. For each architecture three models are provided, each trained on a different scene of MVS dataset.

We first evaluate on the *graffiti* scene in the ACRD dataset. We use the overlapping error mentioned in [8] to find the ground truth correspondences between images. The nearest neighbor distance ratio is used to find matches using descriptors. The nearest neighbor distance ratio is defined as ratio of distance of the nearest neighbor to the second nearest neighbor. Let p be a patch from an image and p' and p'' be its nearest and second nearest neighbor from a second image respectively. Then for a threshold t , (p, p') is consid-

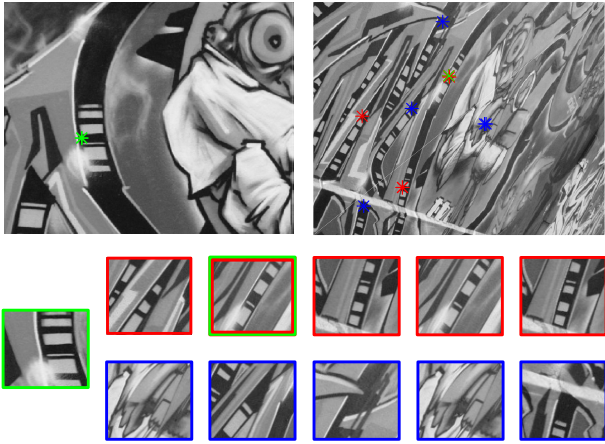


Figure 6. Shows incorrect match by MROGH corrected by our hybrid matching method. The green mark in the left image indicates the point whose correspondence needs to be found in the right image. In the right image, the blue and red points show the nearest neighbors using MROGH and our descriptor respectively. The row of red patches corresponding to the red points, and blue patches corresponding to the blue points. One of the red points in the right image is also marked as green as it is the correct correspondence to the green point in the left image. The patch corresponding to this point is also marked red-green. The top left image is zoomed in for clarity.

ered a match when the ratio of descriptor distance of (p, p') to (p, p'') is less than t .

We have observed that using top 20 neighbors from our model in the hybrid matching algorithm with MROGH gives the best recall for the high precision using nearest neighbor distance-ratio criteria. A comparison between MROGH, SIFT and hybrid matching using our model, DeepDesc [9] and DeepCompare [15] using MROGH, SIFT for high viewpoint variation image pair of the *graffiti* scene in the ACRD dataset is shown in Fig. 8. The corresponding images are shown in Fig. 7. The plots are traced out by varying the threshold on the nearest neighbor distance ratio. The total number of correct correspondences is also considerably higher in our hybrid matching as shown in Table 1. We also see that the hybrid matching using our model also improves the performance of other descriptors like SIFT. For SIFT, using the top 10 neighbors gives the best performance. We have also used the hybrid matching using DeepDesc [9] and MROGH. However, we see a much inferior performance as compared to our model. This observation also justifies our dataset having more geometric variations and training with affine transform pairs.

We also evaluate our model and matching scheme on the fountain-P11 [11] which is a popular wide base line image matching dataset. The dataset is provided with a dense point cloud and a set of high resolution images (2000×3072 pixels). The images used for evaluation is shown in Fig. 9. To



Figure 7. Shows the images from the *graffiti* scene used in evaluation. The left most is viewpoint ‘1’, the middle one is viewpoint ‘2’ and the rightmost is viewpoint ‘3’.

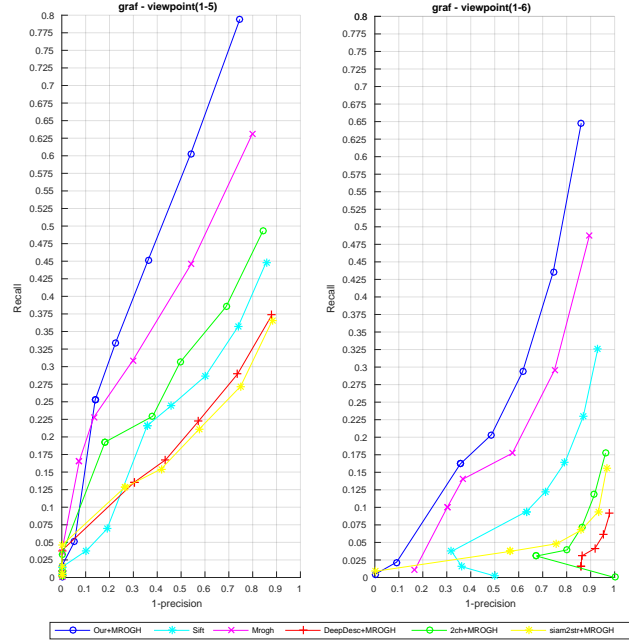


Figure 8. Recall Vs (1-Precision) for various descriptor performances on the oxford graphiti dataset. Left: Viewpoint pair 1 and 5 and right: viewpoint pair 1 and 6.

Method	% Correct Correspondences	
	pair 1-5	pair 1-6
SIFT	44.8	32.6
MROGH	63.0	48.7
DeepDesc [9] + MROGH	37.3	9.1
2-ch [15] + MROGH	49.2	17.7
Siam2Stream [15] + MROGH	36.6	15.5
Ours + SIFT	56.6	44.4
Ours + MROGH	79.4	64.7

Table 1. Shows the percentage of correct correspondences for different descriptors. Our hybrid matching algorithm using MROGH outperforms other methods.

find ground truth correspondence between two images, first hessian affine keypoints are extracted from the images. A 3D point is then projected in both the images and their re-

spective nearest key points lying within 4 pixels radius form correspondence points. Since the images are of high resolution, we scale 128×128 pixels patches to 64×64 pixels for our model and for DeepCompare [15]. For DeepDesc [9], we use 24×24 pixels patches as it provides their best performance.



Figure 9. Shows the images from the *fountain-P11* scene used in evaluation. The left most is viewpoint ‘4’, the middle one is viewpoint ‘7’ and the rightmost is viewpoint ‘8’.

The recall vs (1-precision) curves are shown in Fig. 10 for the wide base line pairs. We see that hybrid matching with our model and MROGH has higher recall through wide range of precision.

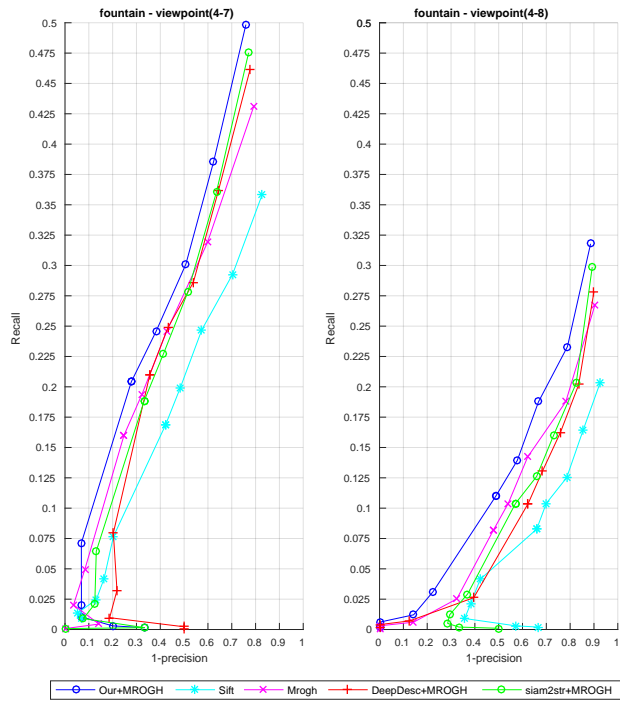


Figure 10. Recall Vs (1-Precision) for various descriptor performances on the p11-fountain dataset. Left: Viewpoint pair 1 and 5 and right: viewpoint pair 1 and 6.

To show that the PS dataset provides more challenging matching and non-matching pairs, we also evaluate DeepDesc and DeepCompare on our the dataset along with our model by comparing their ROC curves used in [12]. We use two of the scenes from test set for evaluation. Images of the scenes are shown in row 4 and 5 of Fig. 1. The scenes

shown in row 4 and 5 are denoted as test scene 1 and test scene 2 respectively. The test set contains equal number of matching and non-matching pairs from each scene. In this evaluation, a given test pair of patches is predicted to be a match (positive) if its distance lies below a threshold and non-match (negative) otherwise. In the ROC curve the true positive rate against the false positive rate are plotted with varying thresholds. It can be observed that many pairs from the MVS data set have small rotation between. To maintain such variation in our test sets, one of the patches from a pair is rotated randomly from $[-\pi/6, -\pi/6]$. The false positive rates of our model and DeepDesc are shown in Table 2. It can be clearly seen that our model outperforms others and has a much lower false positive rate than DeepDesc in both the test scenes. In DeepCompare, among two-stream Siamese networks, the model trained on *liberty* gave the best performance on both test scene 1 and 2. In case two-channel models, the ones trained on *notredame* and *liberty* gave best performance on test scene 1 and 2 respectively. The false positive rates for the models in DeepCompare are close to that of our model in test scene 1 as it is similar to the ones in MVS. In test scene 2 whose content is considerably different from those of MVS, we can see a wider difference in the false positive rates. Also, on test scene 2 the two-channel model has larger false positive rate than the two-stream Siamese model which indicates that the two-channel models are highly over-fitted to their training scenes. The over-fitting issue also causes false positive rate of the two-channel models to increase rapidly beyond a certain threshold.

Method	False Positive Rate (%)	
	Test Scene 1	Test Scene 2
DeepDesc	14.8	26.87
DeepComp-siam2stream(Lib)	6.16	13.19
DeepComp-siam2stream(Not)	7.73	18.91
DeepComp-siam2stream(Yos)	11.63	14.52
DeepComp-2ch(Lib)	5.27	16.41
DeepComp-2ch(Not)	4.93	18.87
DeepComp-2ch(Yos)	6.6	24.44
Ours	3.41	8.17

Table 2. False positive rates at 95% true positive rate. Test scene 1 and 2 refer to the scenes shown in row 4 and 5 in Fig. 1 of our paper. Our model clearly performs better with lower false positive rates.

8. Conclusion

In this paper, we have introduced a new dataset with 15 scenes of varied content and containing images with high

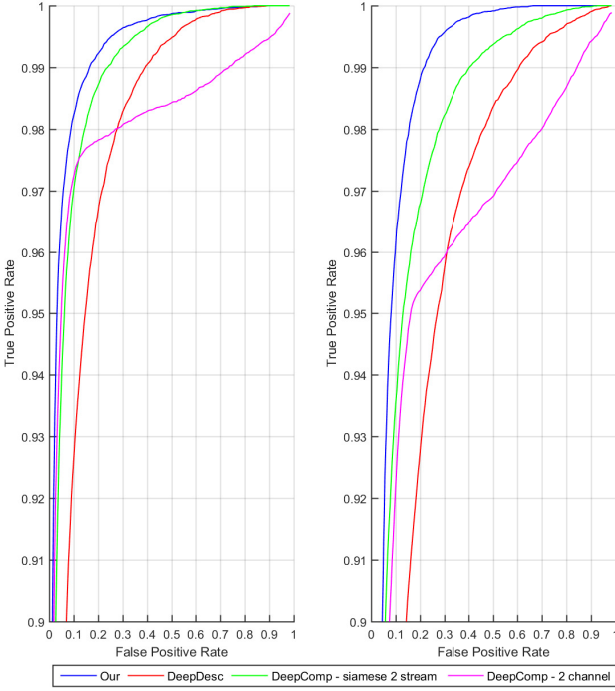


Figure 11. Shows the ROC curve of our model and DeepDesc. The left and the right curves are for scenes shown in row 4 and 5 in Fig. 1 respectively.

geometric transformations. We also train a multi-resolution Siamese network with our dataset and propose a novel hybrid matching technique for finding correspondences that out-performs the state of the art for wide base line matching.

In the future, we want to restrict the usage of heuristic descriptor in our matching by designing a two stage model, where the first model is used for coarse matching and the other (used in place of MROGH) is used for discriminating very small differences in pairs. We want to learn to directly find a set of point correspondences given a pair of images instead of learning descriptors based points extracted by a key-point detector. The advantage here would be that most key-point detectors do not detect points at the exact corresponding points in different images but slightly off which affects the quality of the descriptor.

References

[1] H. Bay, T. Tuytelaars, and L. Van Gool. Surf: Speeded up robust features. pages 404–417, 2006. 1

[2] M. Brown and D. G. Lowe. Automatic panoramic image stitching using invariant features. *Int. J. Comput. Vision*, 74(1):59–73, Aug. 2007. 1

[3] B. Fan, F. Wu, and Z. Hu. Aggregating gradient distributions into intensity orders: A novel local image descriptor. *International Conference on Computer Vision and Pattern Recognition*, 2011. 1

[4] M. Goesele, N. Snavely, B. Curless, H. Hoppe, and S. M. Seitz. Multi-view stereo for community photo collections. *International Conference on Computer Vision*, 2007. 2

[5] R. Hadsell, S. Chopra, and Y. LeCun. Dimensionality reduction by learning an invariant mapping. *International Conference on Computer Vision and Pattern Recognition*, 2:1735–1742. 3, 4

[6] W. He, T. Yamashita, H. Lu, and S. Lao. Surf tracking. *International Conference on Computer Vision*, 2009. 1

[7] D. G. Lowe. Distinctive image features from scale-invariant keypoints. *International Journal of Computer Vision*, 2004. 1, 2

[8] K. Mikolajczyk and C. Schmid. A performance evaluation of local descriptors. *IEEE Transactions on Pattern Analysis and Machine Intelligence*, 2005. 1, 2, 5

[9] E. Simo-Serra, E. Trulls, L. Ferraz, I. Kokkinos, P. Fua, and F. Moreno-Noguer. Discriminative learning of deep convolutional feature point descriptors. *International Conference on Computer Vision*, 2015. 1, 5, 6, 7

[10] N. Snavely, S. M. Seitz, and R. Szeliski. Photo tourism: exploring photo collections in 3d. *ACM SIGGRAPH*, 25:835–846. 1, 2

[11] C. Strecha, W. V. Hansen, L. V. Gool, P. Fua, and U. Thoennessen. On benchmarking camera calibration and multi-view stereo for high resolution imagery. *International Conference on Computer Vision and Pattern Recognition*, 2008. 1, 2, 6

[12] S. Winder, G. Hua, and M. Brown. Picking the best daisy. *International Conference on Computer Vision and Pattern Recognition*, 2009. 1, 2, 7

[13] C. Wu. Visualsfm: A visual structure from motion system, 2011. <http://ccwu.me/vsfm/>. 2

[14] C. Wu, S. Agarwal, B. Curless, and S. M. Seitz. Multicore bundle adjustment. *International Conference on Computer Vision and Pattern Recognition*, 2011. 2

[15] S. Zagoruyko and N. Komodakis. Learning to compare image patches via convolutional neural networks. *International Conference on Computer Vision and Pattern Recognition*, 2015. 1, 5, 6, 7